Pakistan Veterinary Journal

ISSN: 0253-8318 (PRINT), 2074-7764 (ONLINE)
DOI: 10.29261/pakvetj/2026.162

RESEARCH ARTICLE

A multi-target mRNA Vaccine Provides Cross-Prophylactic and Therapeutic Protection Against Diverse *Pasteurellaceae* Infections

Xianguo Yi[1, 2], Shang Liu[3], Yuan Chen[4], Jing Li[3], Mengwei Xu[3], Qing He[3], Rui Liu[3], Tiantian Li[3], Lianshun Wang[3], Bo Li[6], Xi Li[6], Juan Wang[7], Shi Xu[3 *], Tiyun Han[3, 8, 9 *] and Zhengli Chen[1, 5 *]

[1]College of Veterinary Medicine, Sichuan Agricultural University, Chengdu, Sichuan, China; [2]College of Animal Science and Technology, Xinyang Agriculture and Forestry University, Xinyang, Henan, China; [3]Nanjing Chengshi (TheraRNA) Biomedical Technology Co. Ltd., Nanjing, Jiangsu, China; [4]Medical Oncology, Pingxiang People's Hospital, Pingxiang, Jiangxi, China; [5]Laboratory of Experimental Animal Disease Model, College of Veterinary Medicine, Sichuan Agricultural University, Chengdu, Sichuan, China; [6]Rong County Animal Husbandry Service Center, Rongxian Agriculture and Rural Bureau, Zigong, Sichuan, China; [7]School of Foreign Languages, Xinyang Agriculture and Forestry University, Xinyang, Henan, China; [8]School of Life Sciences, Yunnan Normal University, Kunming, Yunnan, China; [9]Engineering Research Center for Valorization of Unique Bio-Resources in Yunnan, Ministry of Education, Kunming, Yunnan, China.
*Corresponding author: xushi@therarna.cn (SX); hantiyun@therarna.cn (TH); chzhli75@163.com (ZC)

ARTICLE HISTORY (26-427)

Received: April 18, 2026
Revised: June 15, 2026
Accepted: June 26, 2026
Published online: July 05, 2026

Key words:
Conserved antigens
Cross-protection
mRNA vaccine
Pasteurellaceae
Prophylactic and therapeutic effect

ABSTRACT

Pasteurellaceae pathogens, including *P. multocida*, pose significant threats to humans, livestock, and poultry, while the effectiveness of antibiotic treatment is gradually being compromised by the problem of antibiotic resistance. Here, we developed a conserved multi-target mRNA vaccine strategy to achieve broad-spectrum prevention and therapy against *Pasteurellaceae* infections. Six highly conserved intracellular antigens, with truncated sequence similarities all exceeding 91%, were selected for the development of a novel mRNA platform against *Pasteurellaceae*. In mouse models, the vaccine conferred strong protection against *P. multocida* and showed cross-protection against four *Pasteurellaceae* pathogens, reducing lung bacterial burden by up to 10-fold compared with the challenge control. In a rabbit acute pneumonia model, the vaccine significantly improved survival by over 40% and reduced lung pathology following *P. multocida* infection. Notably, repeated administration of vaccine exhibited preliminary therapeutic efficacy in naturally infected animals, including one cat, piglets (with a 40% reduction in infection rate), and laying hens (with an approximately 20% increase in egg production), resulting in bacterial burden and alleviation of clinical symptoms. These findings demonstrate that a conserved multi-antigen mRNA vaccine can induce broad-spectrum protective effect against *Pasteurellaceae* pathogens.

To Cite This Article: Yi X, Liu S, Chen Y, Li J, Xu M, He Q, Liu R, Li T, Wang L, Li B, Li X, Wang J, Xu S, Han T and Chen Z, 2026. A multi-target mRNA vaccine provides cross-prophylactic and therapeutic protection against diverse *Pasteurellaceae* infections. Pak Vet J, 46(7): 1678-1694. http://dx.doi.org/10.29261/pakvetj/2026.162

INTRODUCTION

The genus *Pasteurella*, particularly *Pasteurella multocida* (*P. multocida*), represents one of the most important zoonotic pathogens within the *Pasteurellaceae* family (Peng *et al*., 2019). *P. multocida* is widely distributed in nature and colonizes a broad range of hosts, including companion animals, livestock, poultry, and humans (Peng *et al.*, 2018; Peng *et al*, 2019; Akcakavak *et al*, 2024). Transmission typically occurs through direct contact, aerosols, or contaminated environments (Kannangara *et al.*, 2020). Clinically, *P. multocida* infection can lead to respiratory diseases such as pneumonia, atrophic rhinitis, and hemorrhagic septicemia, as well as systemic infections depending on the host (Piorunek *et al.*, 2023). Its broad host range and high pathogenicity make it a major concern in both veterinary and public health contexts.

Current strategies for the prevention and treatment of *P. multocida* infections rely heavily on antibiotics and conventional vaccines. While antibiotic therapy remains the primary countermeasure against veterinary *Pasteurellaceae* infections, clinical efficacy is progressively circumvented by the proliferation of

antimicrobial resistance genes and the pathogen's capacity to establish chronic, biofilm-associated reservoirs (Bourely *et al.*, 2019: Munir *et al.*, 2025). Existing vaccines, including whole-cell vaccine, killed vaccines, live-attenuated vaccines, subunit vaccines, and DNA vaccines, have shown varying degrees of success but are often limited by strong serotype specificity and insufficient cross-protection (Tesfaye *et al.*, 2025). For example, *P. multocida* is classified into multiple serotypes (A, B, D, E, and F) based on capsular polysaccharides, and vaccines targeting a single serotype often fail to protect against others (Mostaan *et al.*, 2020).

The rapid development of mRNA vaccine technology has provided a powerful platform for development of next-generation bacterial vaccines. We previously reported on a novel ionizable lipid-based mRNA vaccine for *Streptococcus pneumoniae* that provides cross-protection against multiple serotypes (Xu *et al.*, 2025). Compared with traditional vaccine approaches, mRNA vaccines offer several advantages, including rapid and flexible antigen selection, scalable manufacturing, and the ability to induce both humoral and cellular immune responses (Whitley *et al.*, 2022; Pardi and Krammer, *et al.,* 2024). Importantly, mRNA vaccines enable intracellular antigen expression, facilitating antigen processing and presentation via major histocompatibility complex (MHC) class I and II pathways (Rijkers *et al.*, 2021). This leads to the activation of T cells and B cells, which are critical for clearing pathogens and establishing long-term immune memory. These features make mRNA vaccines especially attractive for targeting pathogens such as *Pasteurella*, which can establish persistent infections in mucosal tissues.

According to research, several surface-exposed and virulence-associated proteins, such as *Pasteurella multocida* lipoprotein E (plpE), *Pasteurella multocida* toxin (rsPMT or toxA), and surface lipoprotein PmSLP3 have been investigated as subunit vaccine candidates and have demonstrated protective efficacy in *Pasteurella* challenge models (Lee *et al.*, 2012; Doan *et al.*, 2020; Cheng *et al.*, 2023; Fegan *et al.*, 2024). However, these antigens often exhibit sequence variability across strains and species, limiting their utility for cross-protective vaccine design (Wu *et al.*, 2021). In addition to *P. multocida*, other members of the *Pasteurellaceae* family, such as *Mannheimia haemolytica* (*M. haemolytica*), *Haemophilus influenzae* (*H. influenzae*), *Glaesserella parasuis* (*G. parasuis*), and *Avibacterium paragallinarum* (*A. paragallinarum*), are also significant pathogens, causing respiratory and systemic diseases in ruminants, humans, swine, and poultry, respectively (Peng *et al.*, 2018). In our previous work on *Enterobacteriaceae*, we demonstrated that vaccines based on conserved antigens (e.g., PstS and YidR) could provide cross-protection against four pathogenic species across different infection sites (Liu and Xu *et al.*, 2025). Additionally, the mRNA vaccine based on the fusion of PhtD and Ply was shown to be effective in protecting against four different serotypes of *Streptococcus pneumoniae*: serotypes 2, 3, 5, and 19A (Xu *et al.*, 2025). This approach highlights the feasibility of targeting conserved core proteins to achieve broad-spectrum immunity beyond species or strain boundaries. Despite differences in host specificity and disease manifestation of different *Pasteurellaceae* pathogens, *Pasteurellaceae* pathogens share conserved structural components and core genetic features (Christensen and Bisgaard *et al.*, 2018). Therefore, a similar strategy may be applicable for developing universal vaccines against this *Pasteurellaceae* family.

Recent research has focused on identifying conserved antigen targets and developing broad-spectrum vaccines against bacterial infection (He *et al.*, 2022; Liu *et al.*, 2025; Walker *et al.*, 2025). For instance, intracellular proteins involved in essential bacterial processes, such as ribosomal proteins, elongation factors, and molecular chaperones, are highly conserved across species and represent promising targets for universal vaccine development (Kennedy *et al.*, 2018; He *et al.*, 2022; Moustafa *et al.*, 2024). Emerging studies have suggested that such conserved proteins can elicit T cell–mediated immune responses and contribute to bacterial clearance, particularly in intracellular or persistent infections (Kennedy *et al.*, 2018). According to reports, vaccines designed to promote cellular immune responses may therefore offer prophylactic as well as therapeutic benefits (Howlader *et al.*, 2023; Park *et al.*, 2024). By combining multiple conserved epitopes or protein domains into a single construct, such vaccines can broaden immune coverage and reduce the likelihood of immune escape (De Groot *et al.*, 2020). This concept is particularly relevant for *Pasteurellaceae* infections, which can persist in host tissues and evade immune clearance.

The aim of the present study was to develop a broad-spectrum mRNA vaccine targeting six highly conserved intracellular antigens of *Pasteurellaceae* and to systematically evaluate its protective efficacy and cross-protection against different bacteria belonging to *Pasteurellaceae*. Furthermore, our research provides proof-of-concept translational observations of protective effects of an mRNA vaccine across diverse host species.

MATERIALS AND METHODS

Reagents: The lipid components used for LNP preparation comprised the ionizable lipid C14-192, as previously described (Xu *et al.*, 2025), DSPC (06030001100, Sinopeg), β-sitosterol (A10024, Yuanye Bio), and DMG-PEG2000 (06020112402, Sinopeg). Tris-HCl (15568025) and sodium acetate (A59148BA) were purchased from Thermo Fisher Scientific. Ethanol (E7023), Tween-20 (P1379), and sodium chloride (S7653) were obtained from Sigma-Aldrich. RIPA lysis buffer (P0013B) and phosphate-buffered saline (PBS, ST476) were sourced from Beyotime Biotechnology.

Plasmid: The pUC57 vector served as the template. A T7 promoter was positioned upstream of the coding region to drive transcription. The construct further incorporated optimized 5'- and 3'-untranslated regions (UTRs) along with a 110-nt poly(A) tail to enhance mRNA stability and translation efficiency. All antigen sequences were fused at the N-terminus to the Fc region of a porcine Ig-like domain-containing protein (pFc) via a linker (Xu *et al.*, 2025). The C-terminus was engineered to include a linker, a STABILON element to facilitate protein stabilization (Xu *et al.*, 2025). For the VA construct, the pig ARVLP

element (the pig CD80 transmembrane domain, the guinea pig FcγRII cytoplasmic domain, and the pig ITCH WWs domain) was additionally fused to the C-terminus (Xu *et al.*, 2025). All coding sequences were codon-optimized to improve expression efficiency, and synthetic genes were obtained from GenScript. Final plasmids were validated by restriction digestion and Sanger sequencing to confirm sequence accuracy and proper assembly.

mRNA synthesis: Plasmids were linearized by restriction enzyme (BspQI, RE057, Novoprotein) digestion before IVT. mRNA was generated using the T7 High Yield RNA Transcription Kit 2.0 (E332, Novoprotein) with minor modifications, using linearized templates. Cap 1 Capping System (M082, Novoprotein) was incorporated to produce capped mRNA. Following a 6-hour transcription reaction, template DNA was removed, and mRNA was purified by lithium chloride precipitation. RNA concentration and purity were measured using a NanoDrop spectrophotometer (Thermo Fisher Scientific), while integrity was assessed by capillary electrophoresis. Purified mRNA was stored at 4°C.

mRNA-LNP preparation: mRNA encapsulation was performed using C14-192 LNPs via microfluidic mixing, as previously described (Xu *et al.*, 2025). Briefly, C14-192, DSPC, β-sitosterol, and DMG-PEG2000 were dissolved in ethanol at a molar ratio of 45:8:45.5:2 to form the organic phase. The aqueous phase consisted of mRNA diluted in 20mM sodium acetate buffer (pH=5.5). The two phases were combined in a microfluidic device at a flow ratio of 95:5 (aqueous:organic). The lipid-to-mRNA mass ratio was maintained at ~25:1. The resulting formulation was adjusted to physiological pH (7.0-7.4) with Tris-HCl buffer, filtered through a 0.22μm membrane, and stored at 2-8°C. Particle size, polydispersity index (PDI), and zeta potential (ZP) were measured by dynamic light scattering (DLS). Encapsulation efficiency was determined using RiboGreen (R11490, Thermo Fisher Scientific) according to the manufacturer's instructions.

In vitro expression of mRNA: HEK293T cells were seeded in 6-well plates at a density of 8×10^5 cells per well and cultured in MEM supplemented with 10% fetal bovine serum. Cells were transiently transfected with mRNA using LNP3 (Chen *et al.*, 2022). After 48 hours, both culture supernatants and cell lysates were collected. Cells were lysed in RIPA buffer to extract total protein. Protein concentrations were quantified using a BCA assay.

Western blotting: Protein samples (40μg) were mixed with 5 × loading buffer, denatured at 100°C for 5 minutes, and centrifuged at 12,000rpm for 5 minutes at 4°C. Proteins were separated by SDS-PAGE and transferred onto PVDF membranes. A pre-stained protein ladder (BL712A, Biosharp) was used for molecular weight estimation. Membranes were blocked with 5% skim milk for 1 hour at room temperature and incubated overnight at 4°C with rabbit anti-His primary antibody (LF308, Epizyme Biotech) diluted 1:1000 in General Antibody Diluent (PS119L, Epizyme Biotech). After washing with TBST, membranes were incubated with HRP-conjugated goat anti-rabbit IgG secondary antibody (1:5000, LF102, Epizyme Biotech) for 1 hour at room temperature. Following additional washes, signals were detected with Omni-ECL Enhanced Detection Reagent (SQ101L, Epizyme Biotech) and visualized with a ChemiDoc™ imaging system (Bio-Rad, USA).

Animals: The study was approved by the Institutional Animal Care and Welfare Committee of Sichuan Agricultural University, with the approval number DWYXY20250306. All experimental procedures strictly adhered to the AVMA Guidelines for the Euthanasia of Animals. This study was conducted in compliance with the ARRIVE guidelines 2.0. Animals were maintained under controlled environmental conditions with a 12-hour light/dark cycle and relative humidity of 50–60%. Food and water were available ad libitum. All procedures complied with institutional and national guidelines for laboratory animal care and welfare.

For studies involving owned animals (pet cat, piglets, and laying hens), verbal informed consent was obtained from the animal owners prior to inclusion. Written consent was not obtained due to the field-based nature of the study and routine veterinary practice conditions. This approach was reviewed and approved by the Institutional Animal Care and Welfare Committee of Sichuan Agricultural University as part of the overall study protocol.

Animals that had received antibiotic treatment within 14 days prior to enrollment were excluded from the study to avoid confounding effects on bacterial load and clinical outcomes. Sample sizes were determined to ensure adequate statistical power while minimizing animal use, particularly for large animal studies. Randomization was performed using a computer-generated sequence created with the RAND function in Microsoft Excel. Animals were evenly allocated to experimental groups to maintain comparable baseline characteristics. To reduce potential confounding factors, multiple measures were implemented, including randomized treatment allocation, consistent timing of measurements, periodic cage rotation, and blinded outcome assessment. Where blinding was not feasible, this has been explicitly stated. Group allocation was known only to the investigator responsible for randomization at the time of assignment, while personnel involved in animal handling and outcome assessment were blinded to group allocation whenever feasible. Data analysis was performed using coded group identifiers to maintain blinding until completion of statistical evaluation. Biological replicates, defined as independent animals or independently collected samples from separate animals, were used throughout all experiments.

Mice experiment: Female BALB/c mice (6-8 weeks old, 18-25g) were assigned to experimental groups (n=5 or 6 per group) using a computer-generated random number sequence. One no-treatment (NT) group (n=1) was included in each immunization and infection experiment. The total number of experiments was 29 in Fig. 2 and 15 in each of the infection experiments in Fig. 3. A total of 89 mice were used. For challenge experiments involving *P. multocida* (BNCC270568), *G. parasuis* (CVCC4118), and *H. influenzae* (BNCC337544), BALB/c mice (n=6 or

5 per group) were immunized via subcutaneous injection with either sterile PBS or 5μg of the formulated mRNA vaccine on days 0 and 21. On day 35, mice were challenged intranasally after overnight fasting with either 50μL bacterial suspension containing 1×10^7CFU of *P. multocida* or *H. influenzae*, or 40μL containing 5×10^7CFU of *G. parasuis*. For *M. haemolytica* (BNCC376043) infection, every single mouse in each group was given 100μL of PBS or PV (5μg) on days 0 and 21. On day 35, animals were intraperitoneally injected with 500μL of *M. haemolytica* suspension containing 1×10^7CFU per mouse. On day 38, animals were euthanized by intraperitoneal injection of an overdose of pentobarbital sodium (150mg/kg), in accordance with institutional ethical guidelines. Lung tissues were collected for bacterial burden analysis, while additional samples were rinsed with PBS and fixed in 4% paraformaldehyde for hematoxylin and eosin (H&E) staining. Lung histopathological sections were scored on a scale of 0 to 4 based on the severity of inflammatory cell infiltration and alveolar structural damage. 0=normal; 1=minimal (<25% of the field); 2=mild (25–50%); 3=moderate (50–75%); and 4=severe (>75%).

Bacterial load assay: At the experimental endpoint, lung tissues were aseptically harvested from each group. Approximately 10mg of tissue was weighed and transferred into sterile tubes containing 100μL of sterile PBS. Samples were homogenized on ice using a mechanical homogenizer until complete disruption was achieved. The homogenates were subsequently diluted 1:100 in sterile PBS, and 100μL of each dilution was plated onto selective agar. Columbia blood agar was used for *P. multocida*, *M. haemolytica*, and *H. influenzae* (n=6 or 5), while tryptic soy agar (TSA) plates were used for *G. parasuis* (n=5). The absence of colony growth in these controls confirmed assay specificity. All plates were incubated at 37°C for 48 hours, after which colonies were counted and imaged for documentation.

Rabbit experiment: SPF female *New Zealand White rabbits* (*Oryctolagus cuniculus*, outbred strain), weighing 1.5-2.0kg and aged approximately 8-12 weeks, were used in this study. After 3-7 days of acclimatization, rabbits were randomly assigned to three groups: PV-vaccinated (n=5), PBS control (n=6), and an untreated control (NT, n=1). A total of 12 rabbits were used. Each rabbit was individually identified with an ear tag. Every single rabbit in each group received subcutaneous injections of 1 mL PV (20μg) or PBS on days 0 and 21. On day 35, the rabbits in PV- or PBS-vaccinated groups were challenged subcutaneously with 500μL of *P. multocida* (CVCC44408) suspension containing 100CFU. For all invasive procedures, rabbits were gently restrained, and efforts were made to minimize stress and discomfort. Rabbits were then maintained under normal husbandry conditions and monitored for 8 consecutive days for clinical symptoms and survival. On day 43, rabbits were euthanized by intraperitoneal administration of an overdose of pentobarbital sodium (150mg/kg), consistent with AVMA Guidelines for the Euthanasia of Animals. Death was confirmed by the absence of heartbeat and respiration prior to tissue collection. Lung tissues were collected for photographic documentation and pathological analysis. Rabbits that died during the observation period were subjected to the same necropsy procedures.

Cat experiment: This case study was conducted at Nanjing veterinary hospital. A domestic short-haired cat (*Felis catus*), female, aged approximately 2-4 years and weighing ~3-4kg, was enrolled. No control group was included, as this was an exploratory therapeutic case study involving a single clinical patient, and withholding treatment for control purposes was not ethically justified. Targeted next-generation sequencing (tNGS) of nasal swab samples confirmed co-infection with *P. multocida* and *H. influenzae*. The cat received subcutaneous injections of PV (1mL, 20μg) in the left cervical region on days 0, 7, 14, 21, and 28. All procedures were performed by licensed veterinarians. The animal was gently restrained during injections to minimize stress, and no invasive procedures requiring general anesthesia were involved. Clinical condition, including respiratory signs, nasal discharge, and general activity, was monitored throughout the study. Nasal fluid samples were collected at day −7 (prior to vaccination) and day 52 for tNGS analysis to assess pathogen load. No euthanasia was required in this case, as the animal showed progressive clinical improvement.

Piglet experiment: This field study was conducted at a commercial pig farm in Lingqiu County, Datong, Shanxi Province, China. Forty weaned piglets (*Sus scrofa domesticus*, commercial crossbred), aged approximately 4-6 weeks and weighing ~8-10kg, were included. Both male and female piglets were enrolled and evenly distributed between groups. Random sampling of 20 animals was performed, and *P. multocida* infection was confirmed using the *Pasteurella multocida* Universal (PM-U) Nucleic Acid Detection Kit (Fluorescent PCR Method, catalog number RD-D-5611, VIPOTION) with results interpreted as follows: Ct < 40, positive; Ct 40–45, suspected; Ct ≥ 45, negative. The 40 piglets were then divided into two groups (n=20 per group) with comparable infection rates, ages, weights, and genders. Each piglet was individually marked with an ear tag. Each group was housed in separate pens under identical feeding, environmental, and management conditions. Every single piglet in each group received intramuscular injections of 2mL PV (40μg) or PBS in the left neck region on days 0, 5, 10, and 21. Piglets were monitored daily for clinical signs, including coughing, dyspnea, reduced feed intake, and lethargy. Humane endpoints were established in accordance with AVMA guidelines, and animals exhibiting severe distress or moribund condition would be euthanized using an overdose of pentobarbital sodium administered intravenously or intraperitoneally. Pharyngeal swabs were collected on days 0 and 28 for qPCR detection of *P. multocida*. The infection-positive rate was calculated based on Ct values to evaluate the therapeutic efficacy of PV.

Chicken experiment: This experiment was conducted at a poultry farm in Xinzheng, Henan Province, China. Eighteen laying hens (*Gallus gallus domesticus*,

commercial layer breed), aged approximately 20-30 weeks and weighing ~1.5-2.0kg, exhibiting clinical signs of infection were included. Q-PCR analysis was performed using the *Avibacterium paragallinarum* Serovar A/B/C (HPG-A/HPG-B/HPG-C) Nucleic Acid Detection Kit (Triple Fluorescent PCR Method, catalog number MQ-D-6311, VIPOTION), with results interpreted as follows: Ct < 40, positive; Ct 40–45, suspected; Ct ≥ 45, negative. These infected laying hens (n=18) were isolated from the flock and housed separately. An additional 30 age-matched, asymptomatic hens served as NT controls (n=30). Every single laying hen in the treatment group (n=18) received intramuscular injections of 0.5mL PV (10μg) in the leg muscle on days 0, 7, 14, and 21. From day 0 to day 35, animals were monitored regularly for clinical symptoms, including facial swelling, ocular and nasal discharge, respiratory signs, diarrhea, joint swelling, and lameness. Clinical scores were assigned according to standardized scoring criteria. Humane endpoints were defined based on AVMA recommendations, including severe respiratory distress, inability to stand or access food and water, or extreme lethargy. Laying hens meeting these criteria would be humanely euthanized using approved methods, such as intravenous or intracoelomic administration of pentobarbital sodium. Ocular and nasal swabs were collected on days 0 and 28 for qPCR detection of *A. paragallinarum*. Egg production rates were recorded during weeks 2–5 after treatment to comprehensively evaluate vaccine efficacy.

Statistical analysis: Statistical analyses were performed using GraphPad Prism software (version 10.4.0). Data were first assessed for normality and homogeneity of variance. When these assumptions were satisfied, parametric tests were applied. Differences between two groups were analyzed using an unpaired *Student's t*-test, while comparisons among multiple groups were performed using one-way analysis of variance (*ANOVA*) with *Dunnett's* multiple comparisons test. When data deviated from normality (*Shapiro–Wilk* test, P<0.05), the non-parametric *Kruskal–Wallis* test was used for overall group comparisons, followed by *Dunn's* multiple comparisons test for pairwise comparisons against the control group. Alternatively, the nonparametric *Mann–Whitney* test was used. Overall survival was estimated using the *Kaplan–Meier* method. Differences in survival distributions among groups were compared using the log-rank (*Mantel–Cox*) test, as the primary test for equality of survival curves. Values of *P<0.05, **P<0.01, ***P<0.001, and ****P<0.0001 were considered significant.

RESULTS

Multi-antigen fusion mRNA vaccines confer protection against *P. multocida* infection: Within the *Pasteurellaceae* family, *P. multocida* is one of the most common pathogens associated with human infections and is primarily transmitted through animal–human contact (Piorunek *et al.*, 2023). Current vaccine strategies are limited by strong serotype specificity and narrow protection, making it difficult to achieve cross-protection against diverse *Pasteurella* serotypes (Tesfaye *et al.*, 2025). The identification of conserved antigen targets, selection of core epitopes, and multi-target fusion design represent promising approaches for developing broad-spectrum vaccines (Xu *et al.*, 2025; Liu *et al.*, 2025).

In this study, we first selected two previously validated protective antigens, plpE and toxA, from *P. multocida* (Seo *et al.*, 2009; Cheng *et al.*, 2023). Functional antigenic fragments were identified and fused using GS linkers. Structural prediction indicated that the fusion protein forms stable secondary structures with high confidence, as indicated by a predicted template modeling (pTM) score of 0.59 (Fig. 1a and Supplementary Fig. 1a). Furthermore, based on our previous findings in bacterial vaccine studies, elongation factors, molecular chaperones, and ribosomal proteins are highly conserved and functionally essential. Therefore, EF-Tu, dnaK, and EF-G were selected as candidate targets. Based on molecular weight and structural features, domain truncation was performed, and the selected regions were fused into a single construct with a pTM score of 0.58 (Fig. 1b and Supplementary Fig. 1b). Additionally, highly conserved ribosomal proteins were selected, including large subunit protein rplE and small subunit proteins rpsC and rpsE. These proteins underwent similar truncation and fusion to the construct in Fig. 1b and were then subjected to secondary structure prediction, and the pTM score was shown as 0.34 (Fig. 1c and Supplementary Fig. 1c). Together, these designs aimed to generate a multi-target fusion antigen capable of providing effective protection against *P. multocida* infection.

Based on the three fusion antigens described above, three mRNA vaccine constructs were generated: vaccine A (VA), vaccine B (VB), and vaccine C (VC) (Fig. 2a). VA, containing previously validated antigen targets, was designed for secretion to preferentially induce humoral immune responses and served as a reference control. VB encodes the EF-Tu–dnaK–EF-G fusion protein, while VC encodes a larger fusion protein comprising rplE–rpsC–rpsE–EF-Tu–dnaK–EF-G. Both VB and VC were designed for intracellular expression in order to promote cellular immune responses. All fused antigens were incorporated with pFc at the N-terminus and a STABILON (shown as Stab) element at the C-terminus to facilitate protein stabilization (Xu *et al.*, 2025). mRNA integrity analysis by capillary electrophoresis revealed purities of 84.6, 87.8, and 85.2% for VA, VB, and VC, respectively (Supplementary Fig. 2a). In vitro transfection followed by Western blotting confirmed that VA mRNA was successfully expressed and secreted into the culture supernatant, whereas VB and VC mRNAs were efficiently expressed intracellularly (Fig. 2b and Supplementary Fig. 3). These results indicate that the fusion antigens can be effectively translated and properly folded in eukaryotic cells. The three mRNAs were then encapsulated using C14-192 LNPs, which have been validated in pneumococcal mRNA vaccine studies (Xu and Qi, 2025). Particle size analysis showed a uniform distribution between 150–200 nm, with low polydispersity (PDI<0.2) and positive surface charge of +1.20 to +3.20 (Supplementary Fig. 2b and c). The encapsulation efficiency exceeded 85% for all formulations (Supplementary Fig. 2c).

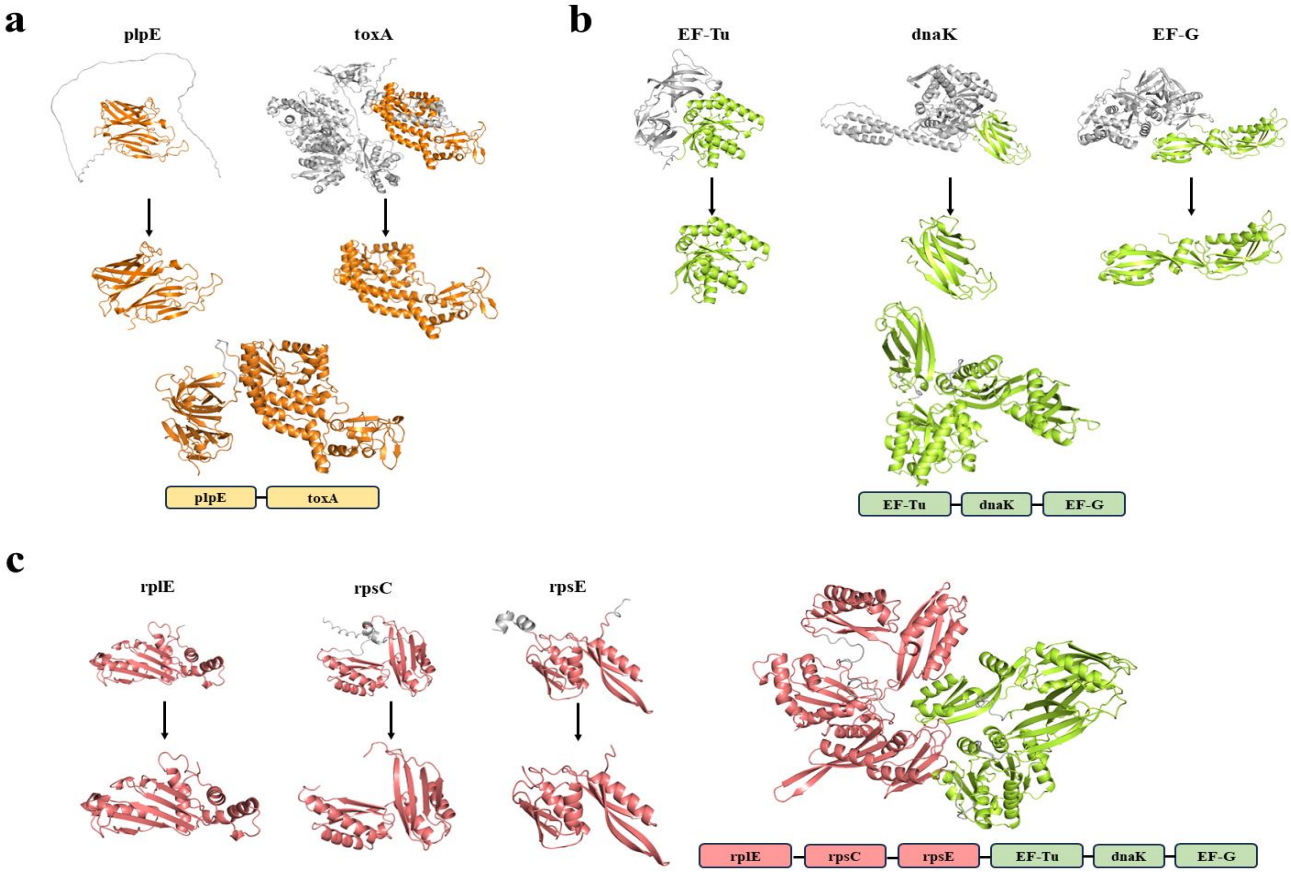

Fig. 1: Truncation and fusion of targeted antigens from *P. multocida*. (a) Schematic of the secondary structure of plpE and toxA, with the truncated domains highlighted in orange. The secondary structure of the plpE-toxA fusion protein was predicted using AlphaFold Server powered by AlphaFold 3. (b) Schematic of the secondary structure of EF-Tu, dnaK, and EF-G, with the truncated domains highlighted in green. The secondary structure of the EF-Tu–dnaK–EF-G fusion protein was predicted using AlphaFold3. (c) Schematic of the secondary structure of rplE, rpsC, and rpsE, with the truncated domains highlighted in pink. The secondary structure of the rplE–rpsC–rpsE–EF-Tu–dnaK–EF-G fusion protein was predicted using AlphaFold3.

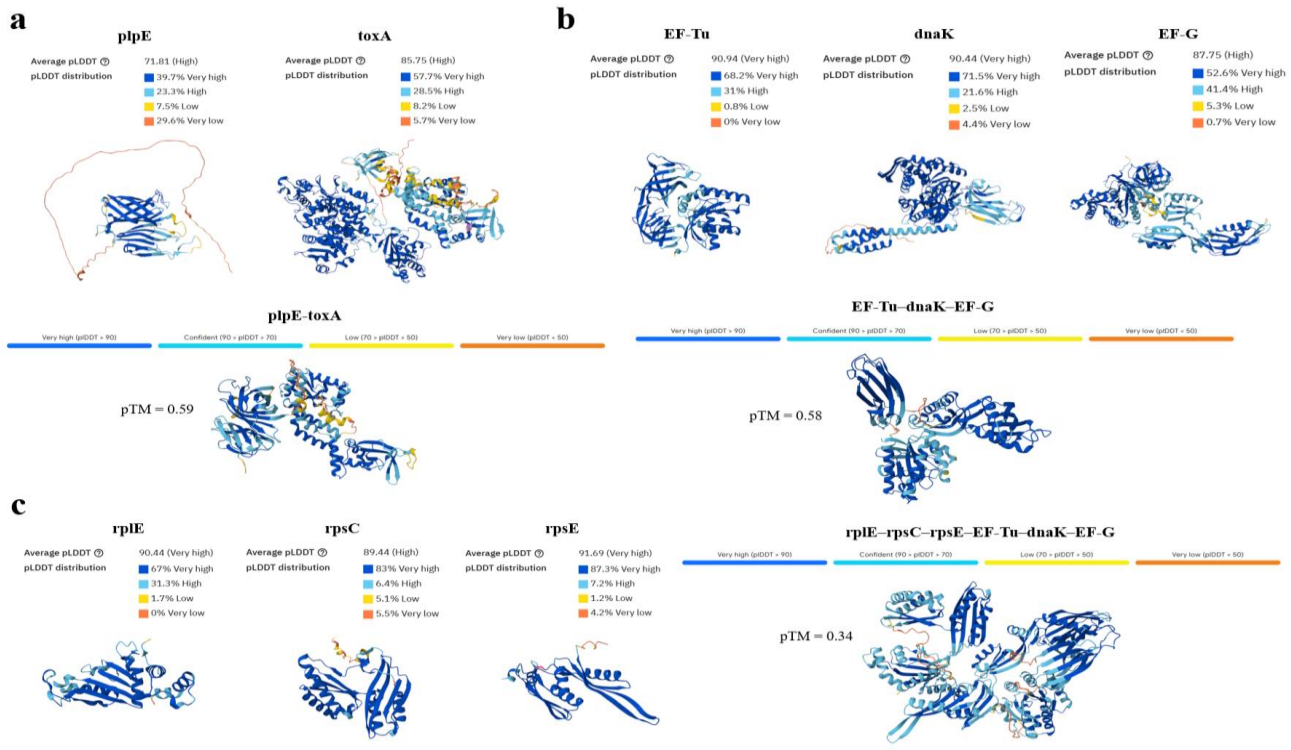

Supplementary Fig. 1: The model confidence of the predicted protein structures of the selected antigens and fused antigens was determined for the development of vaccines. The confidence scores for the individual antigens were downloaded from the AlphaFold database according to their respective UniProt accession numbers and presented as Predicted Local Distance Difference Test (pLDDT) scores. Fused antigens were predicted using AlphaFold Server powered by AlphaFold 3, with predicted template modeling (pTM) scores.

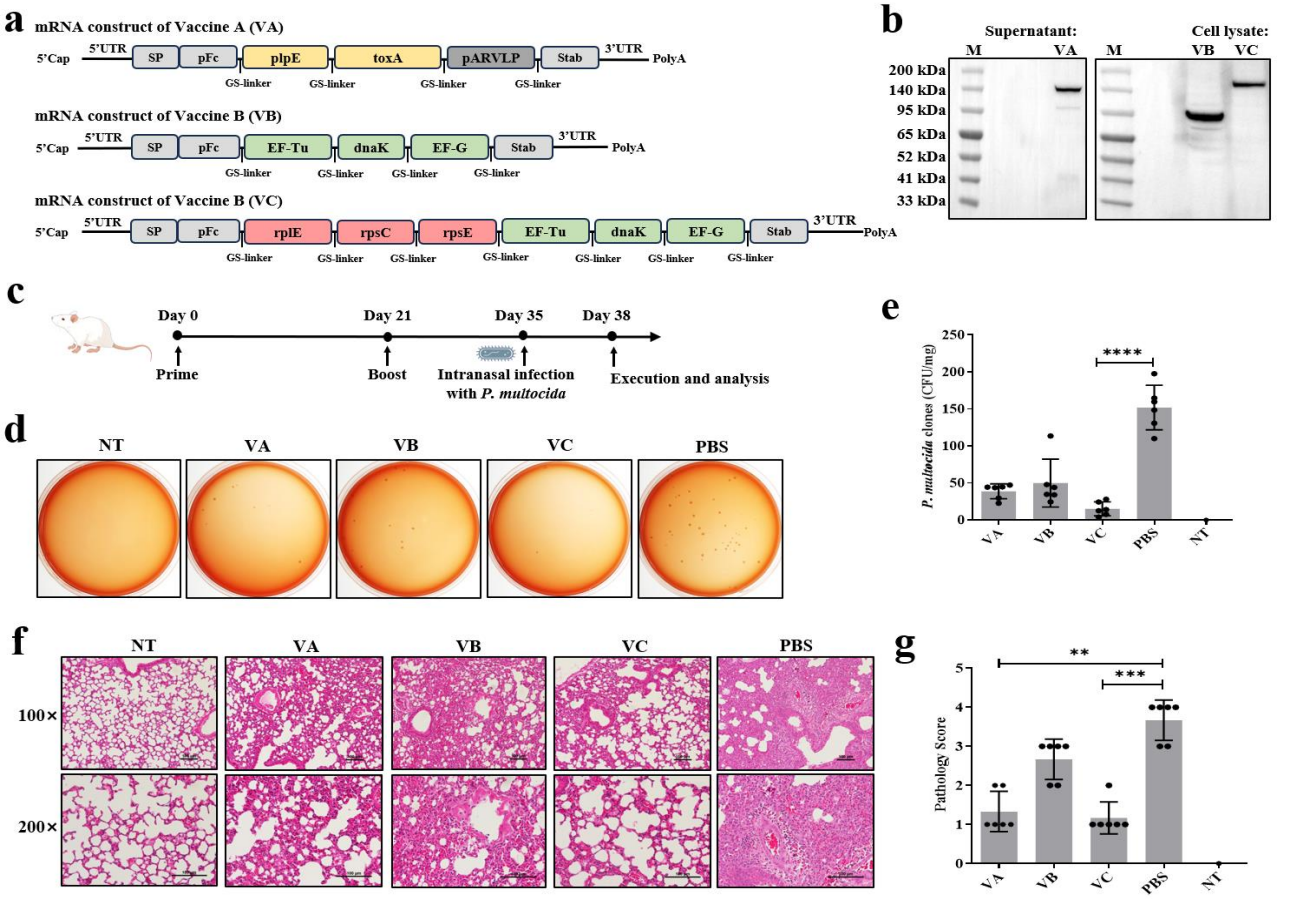

Fig. 2: Development, expression and prophylactic effect of mRNA vaccines against *P. multocida*. (a) Schematic of mRNA construct in developed mRNA vaccines against *P. multocida* infection, with VA serving as a control vaccine. (b) Western blotting analysis of antigens expressed in HEK293T transfected with the indicated mRNA and marker (M). (c) Schematic of vaccination with mRNA vaccines in BALB/c mice followed by intranasal infection with *P. multocida*. Bacterial load assay including (d) representative images and (e) Bacterial colonies in infected lung tissues. (f) Representative pathological capture and (g) pathology score by H&E staining of lung tissues from different groups of mice. There were experimental groups (n=6 per group) and a no-treatment (NT) group (n=1). The representative results in panel e are presented as means ± standard deviation (SD). Error bars represent 95% confidence intervals. Values of **P<0.01, ***P<0.001, and ****P<0.0001 were considered significant. The scale bar in the representative images in panel f is 100μm.

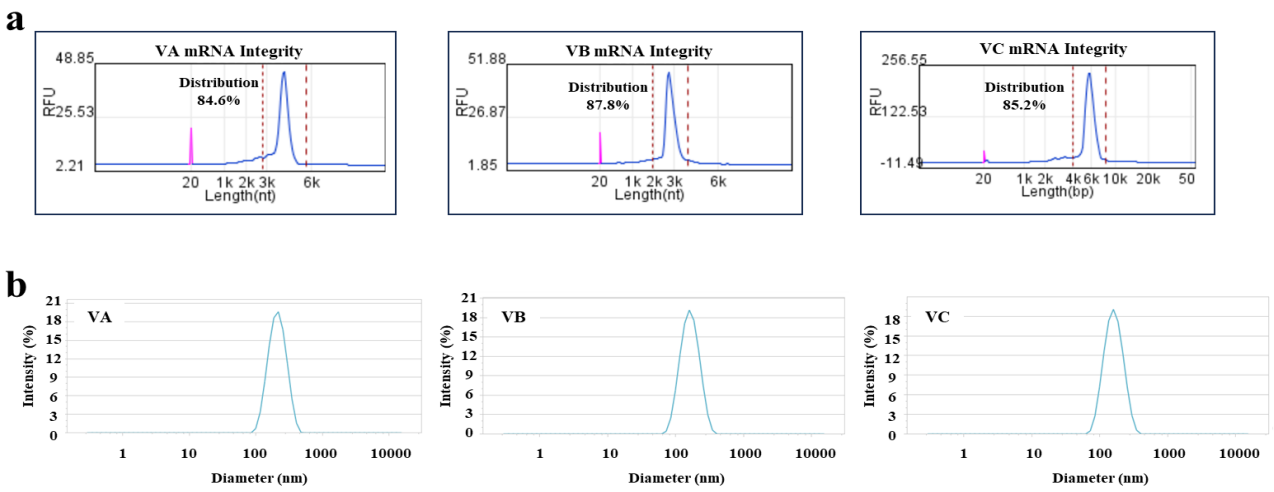

c

mRNA vaccine	LNP	Diameter (nm) ± SD	PDI	ZP (mV) ± SD	Encapsulation Efficiency
VA	C14-192	198.37 ± 44.60	0.131	2.58 ± 0.25	89%
VB	C14-192	168.29 ± 51.87	0.136	1.20 ± 0.18	87%
VC	C14-192	166.66 ± 51.79	0.094	3.20 ± 0.23	90%

Supplementary Fig. 2: Quality control of mRNA vaccines against *P. multocida*. (a) Capillary electrophoresis analysis for the prepared mRNA in vaccines, including VA, VB, and VC. (b) Particle size distribution of the indicated mRNA-LNPs. (c) Summary of the characterization of the indicated mRNA-LNPs, including diameter, PDI, ZP and encapsulation efficiency. Representative results (n=3 or 1) in panel c are presented as means ± SD.

To verify the protective effects of vaccines, mice were immunized subcutaneously with VA, VB, or VC on days 0 and 21 (Fig. 2c). Then, they were challenged intranasally with *P. multocida*. Animals were sacrificed 3 days post-infection for analysis. The lungs of PBS-treated mice exhibited the highest bacterial burden, with an average value of around 150CFU/mg (Fig. 2d and e). In contrast, the VB and VC groups exhibited markedly reduced bacterial loads (p=0.0599 and p=0.1120, respectively). The lowest levels were observed in the VC group at approximately 20CFU/mg. This was significantly different from the PBS group (P<0.0001; Fig. 2d and e). Histopathological analysis of lung tissues revealed severe damage in PBS-treated mice, including marked alveolar septal thickening, loss of alveolar architecture, thickening of bronchial smooth muscle, and extensive inflammatory cell infiltration. In contrast, VA- and VB-immunized mice showed moderate alveolar septal thickening and structural disruption. Notably, VC-immunized mice maintained largely intact alveolar structures, with only mild septal thickening and limited inflammation (Fig. 2f). Further pathological scoring revealed significant differences between the VC and PBS groups (P=0.0005; Fig. 2g).

A novel multi-target mRNA vaccine encoding conserved antigens confers cross-protection against multiple *Pasteurellaceae* pathogens: The *Pasteurellaceae* family comprises multiple pathogenic species capable of infecting humans, livestock, and poultry (Peng *et al.*, 2018). Although these pathogens differ in host range, infection sites, and specific molecular mechanisms, their bacterial structures and core genes are largely conserved (Christensen and Bisgaard *et al.*, 2018). Previously, we developed an *Enterobacteriaceae* vaccine based on sequence homology of two antigen targets, PstS and YidR, derived from *Klebsiella pneumoniae*. This vaccine conferred significant protection against four pathogenic *Enterobacteriaceae* species infecting different tissues (Liu *et al.*, 2025). Based on this rationale, we performed sequence similarity analysis and phylogenetic analysis of six antigen targets (rplE, rpsC, rpsE, EF-Tu, dnaK, and EF-G) using representative full-length amino acid sequences from *P. multocida*, *M. haemolytica*, *H. influenzae*, *G. parasuis*, and *A. paragallinarum* (Supplementary Fig. 4 and 5). As shown in Supplementary Fig. 4, the amino acid sequence identity of these six antigens across the five species was greater than 80%. Notably, five of the antigens, excluding dnaK, showed sequence identities greater than 90%. Further analysis of the truncated antigen sequences revealed that dnaK also exhibited >90% similarity (Fig. 3a). In particular, sequence identity of dnaK between *G. parasuis* and *M. haemolytica* exceeded 99%. Among the truncated regions, EF-Tu sequences from *P. multocida* and *H. influenzae* were identical (100% similarity). Based on these findings, we selected *G. parasuis*, which exhibited relatively high sequence conservation, to construct a new vaccine. Using the same truncation strategy as VC, the six antigen targets were processed and assembled into an identical mRNA construct, designated as the *Pasteurellaceae* vaccine (PV). mRNA integrity analysis showed a purity of 86.3%. The encapsulation efficiency of mRNA-LNPs reached 89%, with a uniform particle size distribution averaging ~150 nm and a positive surface charge of +3.43 (Supplementary Fig. 6).

Further, we evaluated the cross-protective efficacy of PV in mouse infection models using four *Pasteurellaceae* pathogens (*P. multocida*, *G. parasuis*, *H. influenzae*, and *M. haemolytica*). In the *P. multocida* respiratory infection model, PV effectively reduced bacterial colonization in the lungs comparing with the PBS group (~150CFU/mg vs. ~350CFU/mg, P=0.0010; Fig. 3b). PV also significantly alleviated pulmonary inflammation as well as structural damage to alveoli and bronchial epithelium (Fig. 3b). This was confirmed by pathology score (p=0.0317). Similarly, compared with the PBS control group, PV immunization markedly decreased lung infection (from ~20CFU/mg to ~10CFU/mg, p=0.0047) and inflammation caused by *G. parasuis* (Fig. 3c). In the *H. influenzae* respiratory infection model, PV demonstrated comparable antibacterial and protective effects, including reduced bacterial burden (from 1500CFU/mg to ~600CFU/mg, p=0.0041) and improved histopathological outcomes (Fig. 3d). Finally, in a *M. haemolytica* intraperitoneal infection model, PV also conferred significant protection against lung infection (from 100CFU/mg to ~10CFU/mg, P=0.0001) and associated tissue damage (Fig. 3e). Pathological score verified this result (P=0.0013). Collectively, these results demonstrate that PV, developed based on six conserved antigen targets, provides cross-protection against multiple pathogenic species within the *Pasteurellaceae* family.

Previous studies have shown that *P. multocida* has a broad host range that includes cats, dogs, rabbits, poultry, livestock, and other animals (Peng *et al.*, 2018). It is also a zoonotic pathogen. In contrast, *H. influenzae* primarily infects humans, *G. parasuis* mainly affects piglets, and *M. haemolytica* predominantly infects ruminants such as cattle and sheep (Dousse *et al.*, 2008). Therefore, it is necessary to further evaluate the protective efficacy of PV in additional host-specific infection models.

***Pasteurellaceae* mRNA vaccine effectively protects rabbits against *P. multocida* infection:** Clinical investigations indicate that *P. multocida* is one of the most common and threatening pathogens in rabbits, particularly in laboratory and domestic animals (Massacci *et al.*, 2018). In rabbits, infection may lead to rhinitis, otitis media/interna, pneumonia, and reproductive tract infections (Yang *et al.*, 2022). Among these, pneumonia often progresses to severe suppurative pleuropneumonia, characterized by respiratory distress and rapid elevation of body temperature, and represents a major cause of mortality (Michael *et al.*, 2018). To evaluate the protective potential of PV as a proof-of-concept translational observation, we established a rabbit acute pneumonia model induced by subcutaneous infection.

As shown in Fig. 4a, New Zealand White rabbits were subcutaneously immunized with PV on days 0 and 21, followed by subcutaneous challenge with *P. multocida* on day 35. Animals were monitored for 8 consecutive days post-challenge to assess survival. At the study endpoint or upon death, lungs were collected for gross pathological examination (e.g., hemorrhage and swelling) and histopathological analysis to evaluate vaccine-mediated protection. Survival analysis showed that the survival rate in the PBS group was below 20%, whereas

PV immunization increased survival to 60% (p=0.2718; Fig. 4b and Supplementary Table 1). As shown in Fig. 4c, gross examination of lung tissues from rabbits that died during the observation period and those euthanized at the endpoint revealed clear differences among groups. In the NT group, lungs appeared normal, with a pale pink color, uniform texture, and no obvious lesions. In the PV group, lungs from surviving rabbits were close to normal in color and exhibited only mild lesions, whereas lungs from deceased animals showed darker coloration with moderate swelling and congestion. In contrast, rabbits in the PBS group exhibited more severe pathology. Lungs from surviving animals were red with evident congestion, while those from deceased animals appeared dark red to purplish, with pronounced congestion, swelling, and in some cases, signs of necrosis. Overall, the severity of lesions in the PBS group was markedly greater than in the other groups.

Supplementary Table 1: *Kaplan-Meier* survival analysis – number at risk

Time (day)	PV (n=5)	PBS (n=6)	NT (n=1)
0	5	6	1
2	5	6	/
3	4	/	/
5	/	3	/
8	3	1	1

Histopathological analysis further supported these observations (Fig. 4d and e). Lung tissues from the NT group displayed intact architecture, including well-preserved alveoli and bronchi, with no significant inflammatory infiltration or necrosis. In the PV group, lung structure remained largely intact in surviving animals, whereas deceased animals showed widened alveolar septa and partial structural disruption. In the PBS group, surviving animals exhibited mild structural damage, while deceased animals showed pronounced alveolar septal thickening, disrupted architecture, and hemorrhage associated with acute lung injury, indicating severe pathological damage.

***Pasteurellaceae* mRNA vaccine exhibits therapeutic efficacy against established infections:** Currently, infections caused by *Pasteurellaceae* pathogens in companion animals, livestock, and poultry are primarily treated with antibiotics (Cao *et al.*, 2024). Although multi-target mRNA vaccines have demonstrated strong prophylactic efficacy, their therapeutic potential remains unclear. To further evaluate PV's potential as a proof-of-concept translational observation, we conducted a series of preliminary trials in naturally infected one cat, piglets, and chickens under field conditions.

During an epidemiological survey of *Pasteurellaceae* infections in cats, we treated a pet cat with chronic rhinitis using five doses of PV, as a preliminary and anecdotal observation (n=1). Nasal swabs were collected before and after treatment for analysis (Supplementary Fig. 7). tNGS of nasal swabs collected 7 days prior to the first immunization revealed co-infection with *P. multocida* and *H. influenzae*, with *P. multocida* showing the highest gene copy number (Supplementary Table 2). Notably, 24 days after the final immunization, neither pathogen was detectable in nasal swabs. These findings provide preliminary evidence supporting a therapeutic effect of PV.

Supplementary Table 2: The tNGS data from the nasal of infected and vaccinated cat that was detected at different time

	Bacterial type	Species name	Number sequences	of Confidence
tNGS data from nasal swab taken on day -7	G-	*Pasteurella multocida*	4848	99%
	G-	*Helicobacter pylori*	35	99%
	G-	*Haemophilus influenzae*	14	99%
	G+	*Streptococcus dysgalactiae*	6	99%
tNGS data from nasal swab taken on day 52	G+	*Streptococcus dysgalactiae*	11	99%

To further evaluate therapeutic efficacy, a field study was conducted at a commercial pig farm in Datong, Shanxi. Among 40 piglets, 20 were randomly selected for laryngeal swab qPCR testing, revealing that 75% were infected with *P. multocida*. The 40 piglets were then evenly divided into two groups: one group received four doses of PV, while the control group received PBS. Laryngeal swabs were collected 28 days after the final immunization for analysis (Fig. 5a). qPCR results showed that most PV-treated piglets reached the Ct detection limit on day 28, indicating reduced bacterial burden and a significant difference compared with the PBS group (P=0.0040; Fig. 5b). The infection-positive rate decreased from 70% to 30% in the PV-treated group, whereas it increased from 80% to 85% in the untreated group (Fig. 5c). These results demonstrate that the mRNA vaccine also exerts therapeutic effects in piglets infected with *P. multocida*.

In parallel, 18 laying hens infected with *A. paragallinarum* and exhibiting severe symptoms of infectious coryza were identified at a poultry farm in Xinzheng, Henan. These laying hens were isolated from the flock and individually housed for treatment. PV was administered four times on days 0, 7, 14, and 21. Combined ocular and nasal swabs were collected on days 0 and 28, and egg production rates were recorded from weeks 2 to 5 (Fig. 5d). In addition, 30 asymptomatic hens were included as controls. Clinical symptoms were scored according to the criteria listed in Supplementary Table 3. In infected hens, clinical symptom scores began to decline markedly from day 8 after the first vaccination (Fig. 5e and Supplementary Table 4). From day 15 to the study endpoint, treated hens exhibited clinical conditions comparable to those of healthy controls. qPCR analysis of ocular and nasal swabs showed significantly increased Ct values following PV treatment, indicating reduced bacterial loads in both sites (Fig. 5f). Notably, asymptomatic hens also exhibited relatively high Ct values at day 0, which further increased by day 28. Egg production rates in treated hens increased from 28.6% to 49.1% between weeks 2 and 5, reaching levels comparable to those of the non-treated healthy group (Fig. 5g and Supplementary Table 5). These results indicate that PV is also effective for the treatment of *Pasteurellaceae* infection in poultry.

Supplementary Table 3: Clinical scoring criteria for infectious coryza in chickens

Clinical Sign and Description	Severity	Score
Nasal Discharge		
Normal, no discharge	-	0
Small amount of nasal discharge upon pressing the nostril	+ (Mild)	1
Partial or intermittent nasal discharge, or fresh exudate visible adhering to/dried near the nostril	++ (Moderate)	2
Small amount of nasal discharge flows freely without pressing	+++ (Severe)	3
Ocular Discharge		
Normal, no discharge	-	0
Periorbital area filled with clear ocular discharge	+ (Mild)	1
Partial ocular discharge, with recent exudate adhering to adjacent skin surface	++ (Moderate)	2
Continuous or intermittent free-flowing ocular discharge	+++ (Severe)	3
Facial Swelling		
Normal, no swelling	-	0
Unilateral or bilateral swelling of the infraorbital sinus (triangular fossa)	+ (Mild)	1
Unilateral or bilateral sinus swelling with elevation of facial/orbital surface	++ (Moderate)	2
Bilateral swelling with prominent raised mass on facial/orbital surface	+++ (Severe)	3
Conjunctival Congestion		
Normal, no congestion	-	0
Slight redness of conjunctival surface	+ (Mild)	1
Rose-red coloration of conjunctival surface	++ (Moderate)	2
Markedly deep red coloration of conjunctival surface	+++ (Severe)	3

Supplementary Table 4: Clinical symptom scoring during vaccine treatment of infectious coryza in chickens

	Time	D1	D3	D8	D11	D15	D19	D23	D26	D30	D34
PV	Footnote										
(n=18)	49-1	1	1	3	0	0	2	2	1	1	0
	51-1	5	1	0	2	0	0	0	0	1	0
	52-1	4	2	2	0	0	0	0	1	0	0
	56-1	2	2	0	0	0	0	0	1	1	0
	60-1	3	1	2	2	2	2	3	0	1	3
	68-1	1	1	1	0	0	0	0	0	0	0
	69-1	0	0	0	3	0	0	0	0	0	0
	73-1	3	2	0	0	0	1	0	0	0	0
	74-1	4	2	0	0	0	0	0	0	0	0
	76-1	5	3	0	0	0	0	0	1	0	0
	77-1	2	2	0	1	1	0	0	0	0	0
	78-1	2	1	0	1	0	0	0	0	0	0
	82-1	0	0	0	0	0	0	1	0	1	0
	85-1	1	0	0	0	0	0	0	1	0	0
	87-1	4	3	0	0	0	0	0	0	0	0
	94-1	4	3	0	0	0	0	0	0	0	0
	95-1	3	2	0	1	1	0	1	0	0	2
	99-1	2	1	0	0	0	0	0	0	0	0
	Average score	2.56	1.50	0.44	0.56	0.22	0.28	0.39	0.28	0.28	0.28
NT	Footnote										
(n=30)	1	0	0	0	0	0	0	0	0	0	0
	2	0	0	0	0	0	0	0	0	0	0
	3	0	0	0	0	0	0	0	0	0	0
	4	0	0	0	0	0	0	1	0	0	0
	5	0	0	0	0	0	0	1	0	0	0
	6	0	0	0	1	0	0	0	0	0	0
	7	0	0	0	0	1	2	2	1	1	2
	8	0	0	0	0	0	0	0	0	0	0
	9	0	0	0	0	0	0	0	0	0	0
	10	0	0	0	0	0	0	1	0	0	0
	11	0	0	0	0	0	0	1	0	0	0
	12	0	0	0	1	1	0	0	0	0	0
	13	0	0	0	0	0	3	2	2	1	4
	14	0	0	0	0	0	1	0	0	0	0
	15	0	0	0	0	0	0	0	0	0	0
	16	0	0	0	1	0	1	0	0	1	0
	17	0	0	0	0	0	0	0	0	0	1
	18	0	0	0	0	0	0	0	0	0	0
	19	0	0	0	0	0	0	0	0	0	0
	20	0	0	0	0	0	0	0	0	0	0
	21	0	0	0	0	0	0	0	0	0	0
	22	0	0	0	2	2	0	1	1	1	0
	23	0	0	0	0	0	0	0	0	0	0
	24	0	0	0	0	0	0	0	0	0	0
	25	0	0	0	0	0	0	0	1	0	0
	26	0	0	0	0	0	0	0	0	0	0
	27	0	0	0	0	0	0	0	0	0	0
	28	0	0	0	0	0	0	0	1	0	0
	29	0	0	0	0	0	0	0	0	0	0
	30	0	0	0	2	0	0	1	0	0	0
	Average score	0.00	0.00	0.00	0.23	0.13	0.23	0.33	0.20	0.13	0.23

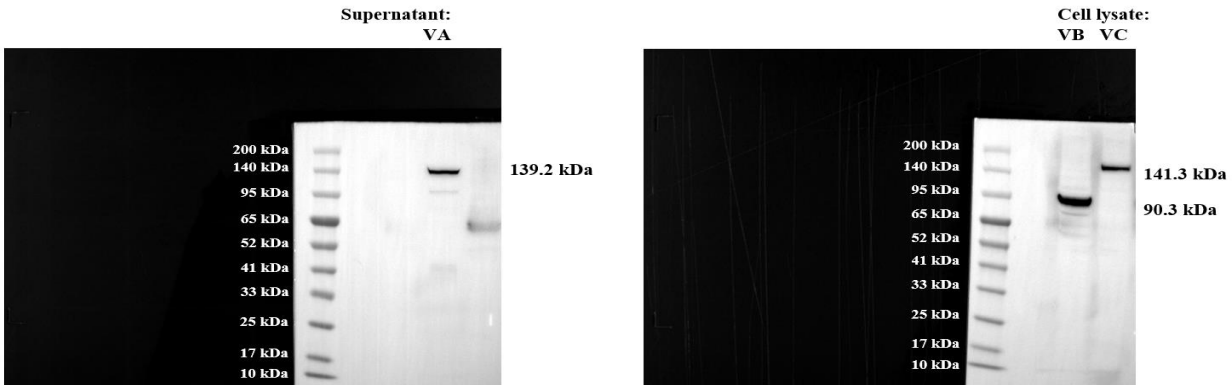

Supplementary Fig. 3: Western blotting analysis of antigens expressed in HEK293T transfected with the indicated mRNA (VA, VB and VC).

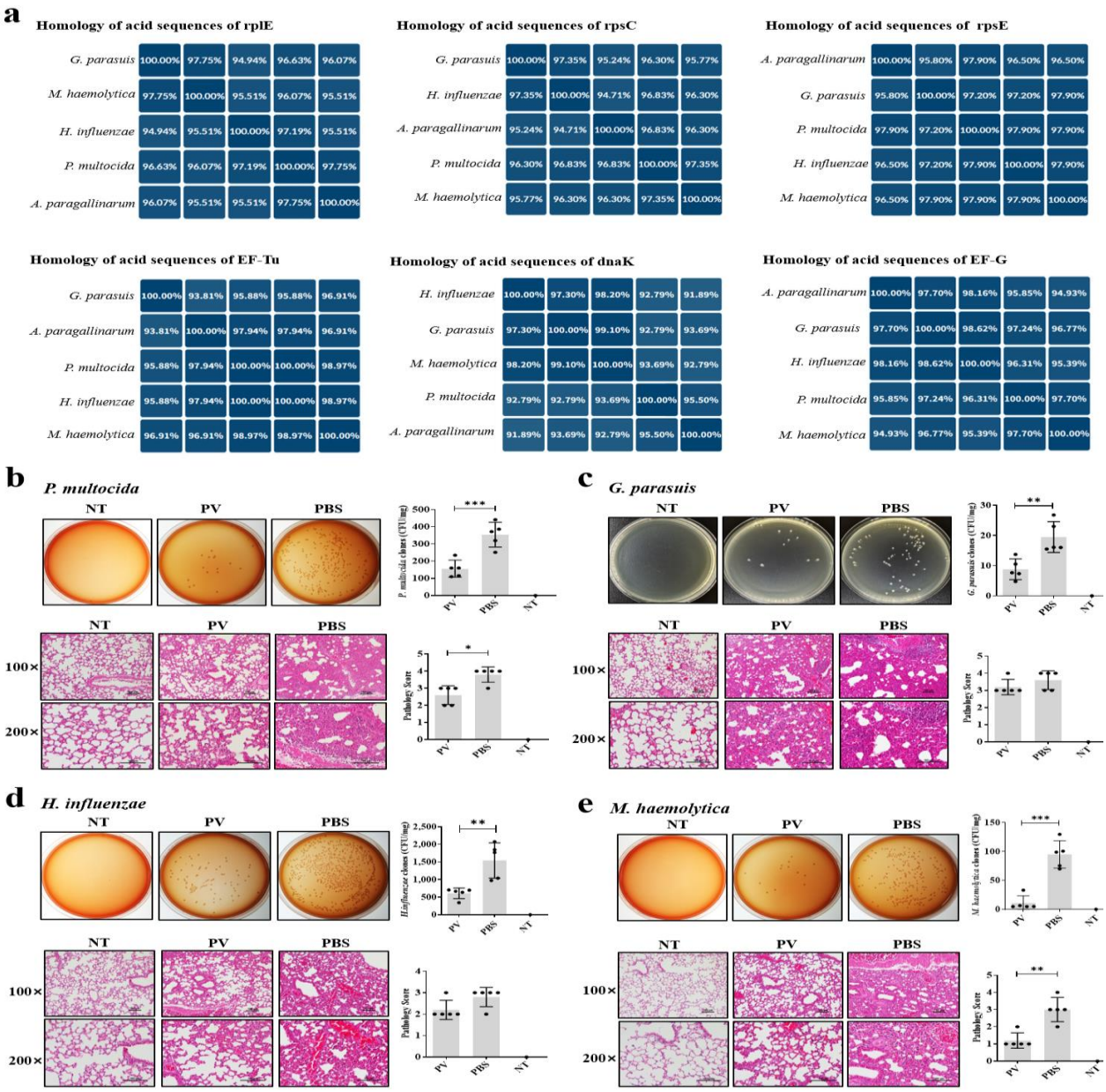

Fig. 3: The prophylactic effect of the developed mRNA vaccine against multiple *Pasteurellaceae* infections in mice. (a) Alignment analysis of representative amino acid sequences of truncated EF-Tu, dnaK, EF-G, rplE, rpsC, and rpsE from *P. multocida*, *M. haemolytica*, *H. influenzae*, *G. parasuis*, and *A. paragallinarum*. (b-d) Bacterial load assay and pathological analysis of lungs of mice vaccinated with the indicated mRNA vaccines or PBS and intranasally infected with (b) *P. multocida*, (c) *G. parasuis*, or (d) *H. influenzae*. (e) Bacterial load assay and pathological analysis of lungs of mice vaccinated with the indicated vaccines and intraperitoneally infected with *M. haemolytica*. There were experimental groups (n = 5 per group) and a no-treatment (NT) group (n = 1). Representative results of the number of bacterial clones are presented as means ±SD. Error bars represent 95% confidence intervals. Values of *P<0.05, ** P<0.01, and ***P<0.001 were considered significant. The scale bar in the representative pathological analysis images is 100μm.

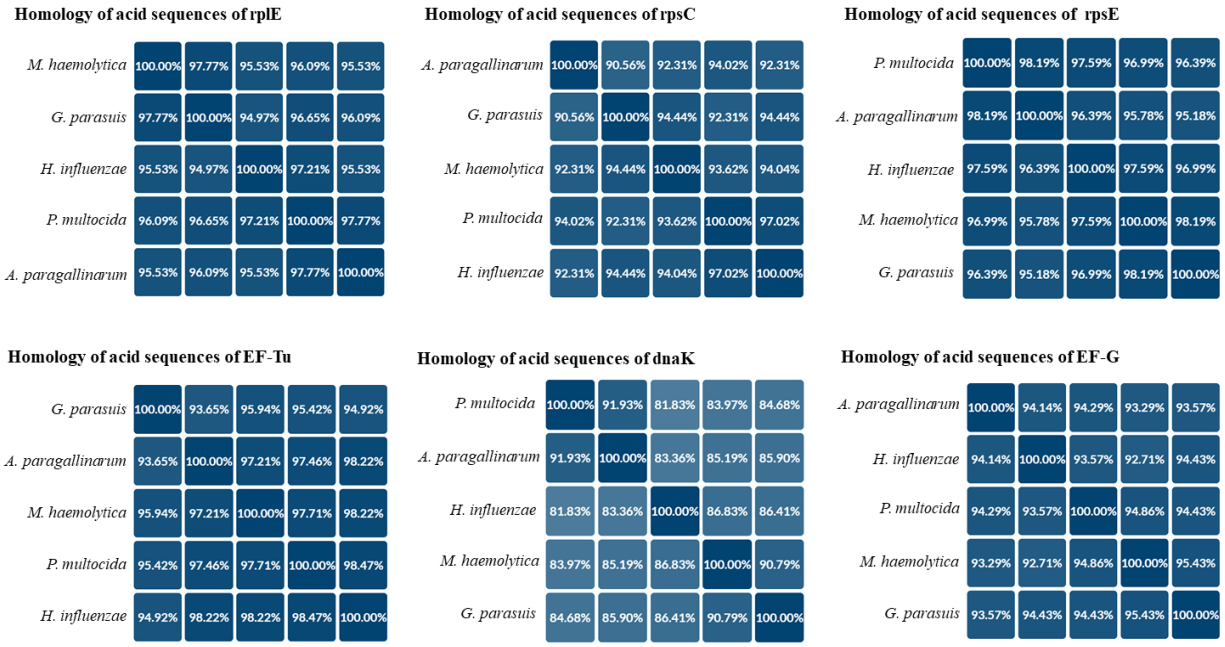

Supplementary Fig. 4: Alignment analysis of representative full-length amino acid sequences of EF-Tu, dnaK, EF-G, rplE, rpsC, and rpsE from *P. multocida*, *M. haemolytica*, *H. influenzae*, *G. parasuis*, and *A. paragallinarum*.

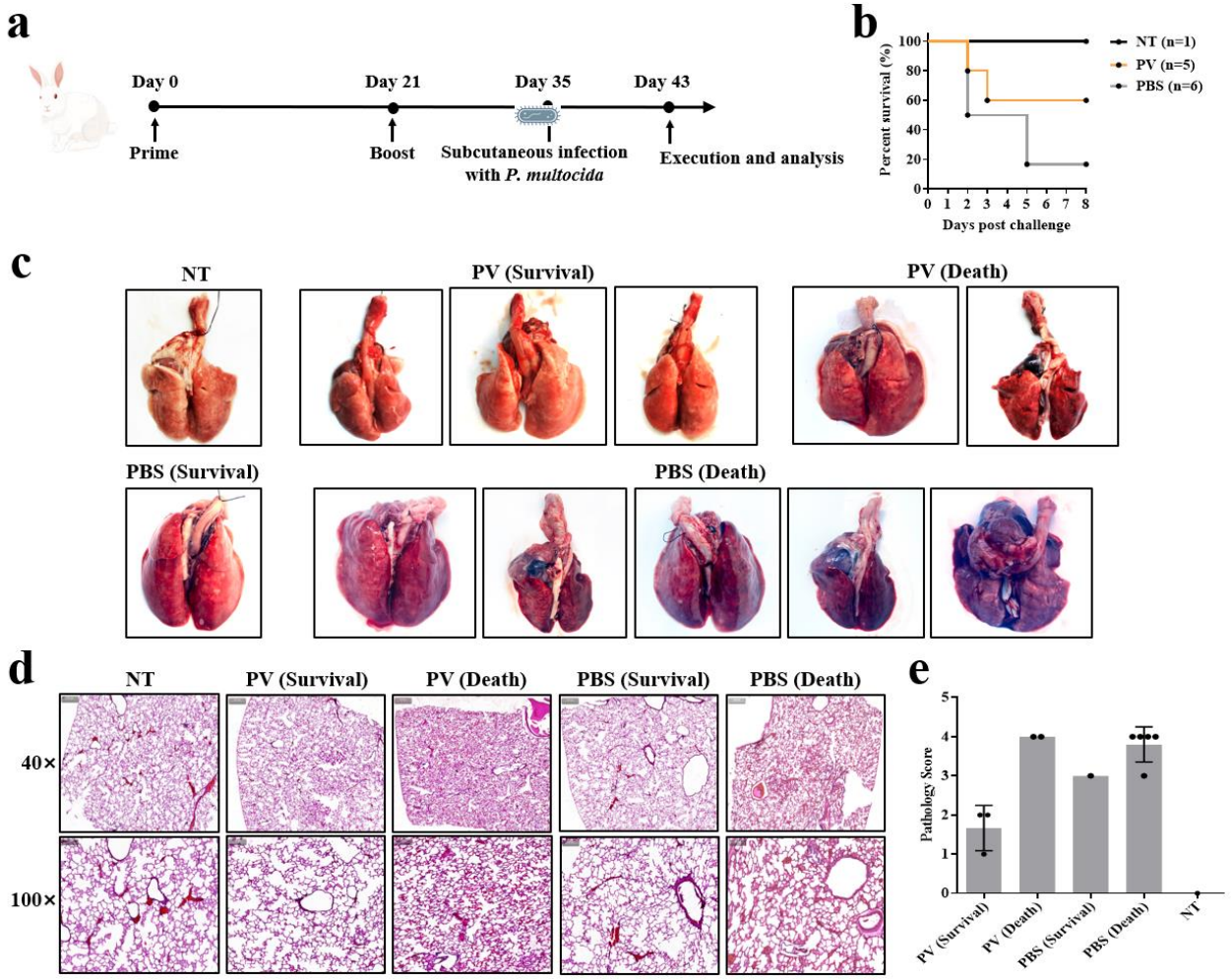

Fig. 4: The prophylactic effect of mRNA vaccine against *P. multocida* infections in rabbits. (a) Schematic of vaccination with the indicated mRNA vaccine in *New Zealand White rabbits*, followed by subcutaneous infection with *P. multocida*. (b) Differences in survival distributions among groups were compared using the log-rank (*Mantel–Cox*) test. (c) Representative captures of the entire lung from different groups of mice. (d) Representative pathological capture and (e) pathology score by H&E staining of lung tissues from rabbits. Rabbits were randomly assigned to three groups: PV-vaccinated (n = 5), PBS control (n = 6), and untreated control (NT, n = 1). The scale bar in the representative H&E images in panel d is 500μm (40×) or 200μm (100×).

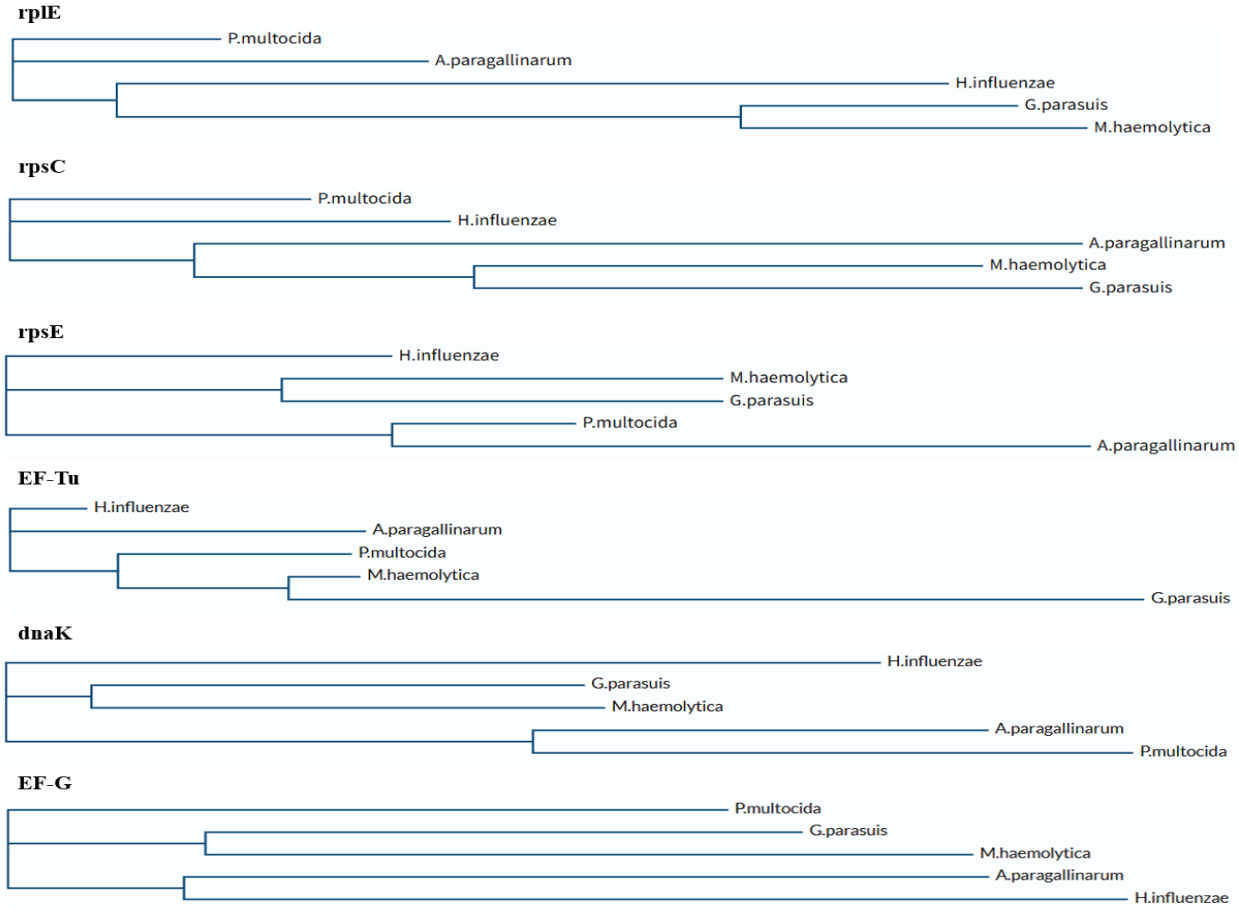

Supplementary Fig. 5: Phylogenetic analysis of representative full-length amino acid sequences of EF-Tu, dnaK, EF-G, rplE, rpsC, and rpsE from *P. multocida*, *M. haemolytica*, *H. influenzae*, *G. parasuis*, and *A. paragallinarum*.

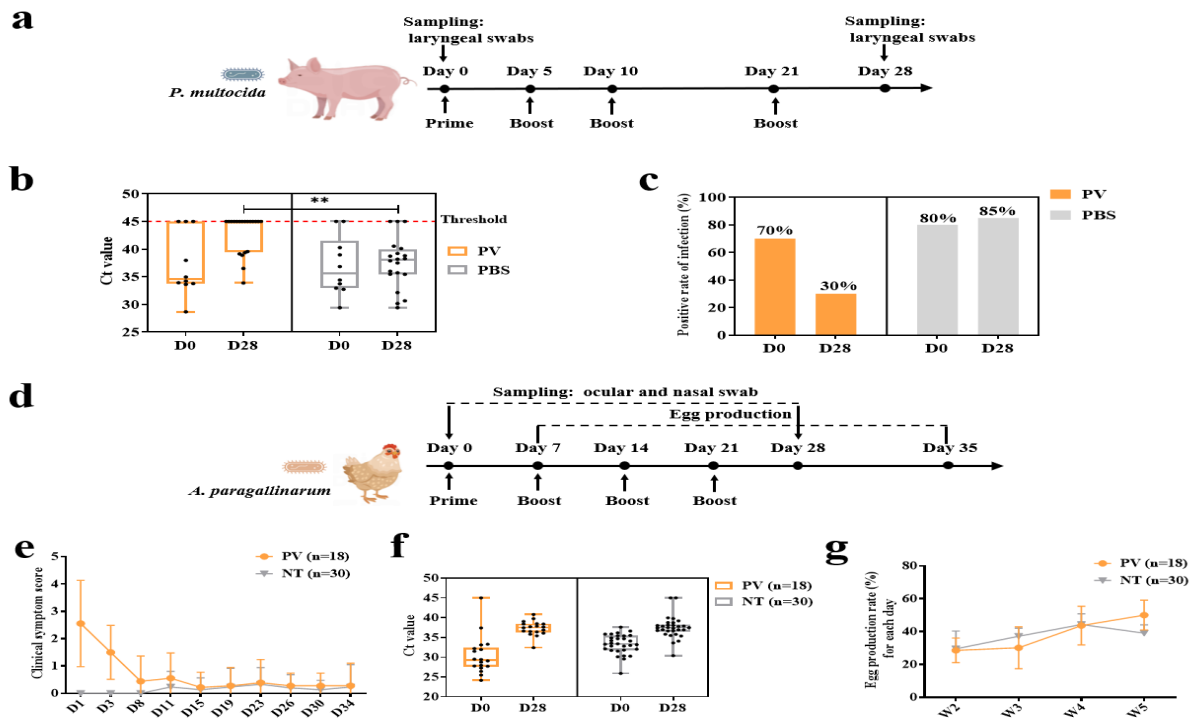

Fig. 5: The therapeutic effect of mRNA vaccine on pigs infected with *P. multocida* and chickens infected with *A. paragallinarum*. (a) Schematic of the indicated mRNA vaccine vaccination and sampling in piglets infected with *P. multocida*. (b) Cycle threshold (Ct) values detected by qPCR for samples from laryngeal swabs collected from *P. multocida*-infected and PV- or PBS- vaccinated piglets (n = 10 on day 0; n = 20 on day 28). (c) The calculated infection-positive rate according to the Ct values in panel b. (d) Schematic of vaccination, sampling, and recording of egg production condition in laying hens infected with *A. paragallinarum* (n = 18) or not (n = 30). (e) The change in average clinical symptom score of laying hens with infectious coryza from day 1 to day 34. (f) Ct values detected by qPCR for samples from ocular and nasal swabs collected from infected and vaccinated, or normal laying hens. (g) The egg production rates for each day from weeks 2 to 5 (n = 7). Representative results in panels b, e and f are presented as means ±SD. Error bars represent 95% confidence intervals. Values of **P<0.01 was considered significant.

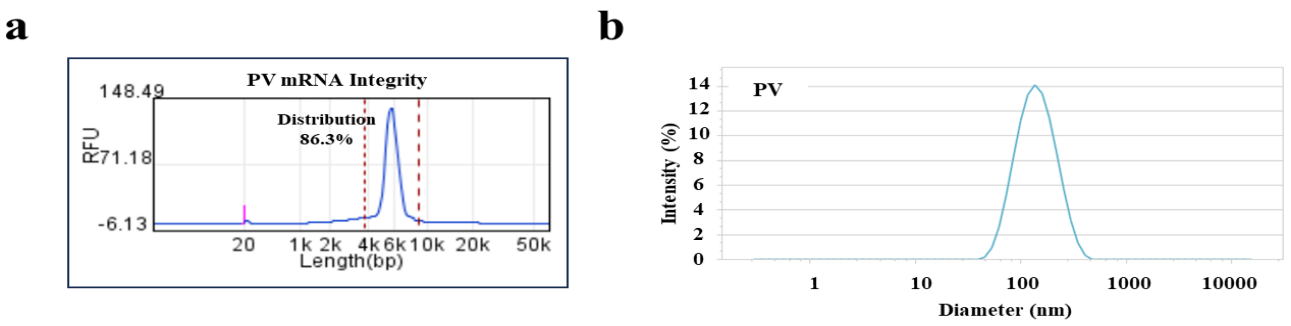

c

mRNA vaccine	LNP	Diameter (nm) ± SD	PDI	ZP (mV) ± SD	Encapsulation Efficiency
PV	C14-192	150.37 ± 53.75	0.138	3.43 ± 0.27	89%

Supplementary Fig. 6: Quality control of mRNA vaccine against multiple *Pasteurellaceae* infections. (a) Capillary electrophoresis analysis for the prepared mRNA in PV. (b) Particle size distribution of the indicated mRNA-LNPs. (c) Summary of the characterization of the indicated mRNA-LNPs, including diameter, PDI, ZP and encapsulation efficiency. Representative results (n = 3 or 1) in panel c are presented as means ± SD.

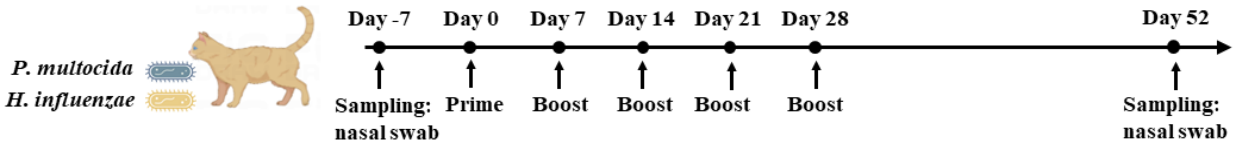

Supplementary Fig. 7: Schematic of the therapy for a pet cat infected with *P. multocida* and *H. influenzae*, and sampling (n = 1).

Supplementary Table 5: Summary of egg production rates during vaccination treatment for infectious coryza in chickens

		Egg production number		Egg production rate for each day		Average egg production rate	
		PV	NT	PV	NT	PV	NT
Time		n=18	n=30	n=18	n=30	28.6%	29.5%
Week 2	D8	4	6	22.22%	20.00%		
	D9	6	7	33.33%	23.33%		
	D10	5	14	27.78%	46.67%		
	D11	3	13	16.67%	43.33%		
	D12	6	7	33.33%	23.33%		
	D13	5	7	27.78%	23.33%		
	D14	7	8	38.89%	26.67%		
Week 3	D15	2	10	11.11%	33.33%	30.2%	37.1%
	D16	3	12	16.67%	40.00%		
	D17	6	10	33.33%	33.33%		
	D18	5	14	27.78%	46.67%		
	D19	6	11	33.33%	36.67%		
	D20	8	11	44.44%	36.67%		
	D21	8	10	44.44%	33.33%		
Week 4	D22	4	12	22.22%	40.00%	43.7%	44.3%
	D23	7	12	38.89%	40.00%		
	D24	8	11	44.44%	36.67%		
	D25	8	16	44.44%	53.33%		
	D26	11	15	61.11%	50.00%		
	D27	9	15	50.00%	50.00%		
	D28	8	12	44.44%	40.00%		
Week 5	D29	6	12	33.33%	40.00%	50.0%	39.0%
	D30	9	10	50.00%	33.33%		
	D31	8	10	44.44%	33.33%		
	D32	10	11	55.56%	36.67%		
	D33	9	12	50.00%	40.00%		
	D34	11	13	61.11%	43.33%		
	D35	10	14	55.56%	46.67%		

DISCUSSION

In this study, we developed a multi-target mRNA vaccine strategy against *Pasteurellaceae* pathogens by integrating prior knowledge of conserved antigen selection with rational fusion design. Building on our previous work in mRNA vaccines against *Enterobacteriaceae*, where conserved antigens enabled cross-protective immunity, we identified six highly conserved intracellular targets (rplE, rpsC, rpsE, EF-Tu, dnaK, and EF-G) across multiple *Pasteurellaceae* species, including *P. multocida*, *M. haemolytica*, *H. influenzae*, *G. parasuis*, and *A. paragallinarum* (Liu *et al.*, 2025). These targets were assembled into fusion constructs and delivered via an optimized LNP-based mRNA platform (Xu *et al.*, 2025). Systematic evaluation in murine models demonstrated robust protection against multiple *Pasteurellaceae* pathogens. Moreover, the vaccine also showed efficacy in a rabbit pneumonia model, and its potential was explored through three proof-of-concept translational observations. Together, these findings establish a conserved multi-antigen mRNA strategy that enables both prophylactic and therapeutic benefits.

Current prevention and treatment strategies for *Pasteurellaceae* infections rely largely on antibiotics and, in some cases, inactivated or subunit vaccines (Tesfaye *et al.*, 2025). However, these approaches are often limited by serotype specificity, incomplete protection, and the growing risk of antimicrobial resistance. Recent advances in mRNA vaccine technology have enabled rapid antigen design, flexible manufacturing, and the induction of both humoral and cellular immune responses. Compared with traditional vaccines, mRNA vaccines encoding conserved multi-target antigens offer key advantages, including broader antigen coverage and the potential to overcome serotype restrictions (Pardi *et al.*, 2024). In the present study, we developed an mRNA vaccine encoding six conserved antigen targets, with the stability brought by pFc and STABILON elements and the delivery by C14-192 LNP (Xu *et al.*, 2025; Xu *et al.*, 2025). These targets are intracellular proteins that are not secreted. Therefore, they are postulated to primarily elicit cell-mediated immune responses against infected cells. However, cell lysis that occurs during acute infection may release these antigens into the extracellular environment, exposing them to the humoral immune system.

Vaccines that predominantly elicit antibody responses, like plpE and toxA antigens, typically confer protection through humoral response (Seo *et al.*, 2009; Cheng *et al.*, 2023). These vaccines are generally effective for prophylaxis (Weerarathna *et al.*, 2024; Khan *et al.*, 2024). However, such approaches are often insufficient for treating chronic bacterial infections due to the relatively short half-life of antibodies and the difficulty of clearing intracellular bacteria. In contrast, vaccines that stimulate cellular immunity may act more slowly but are better suited for clearing intracellular or persistent pathogens through activation of T cell response (Tian *et al.*, 2022; Park *et al.*, 2024). According to reports, intracellular expression of mRNA-encoded antigens facilitates processing via the MHC class I and II pathways, thereby activating cellular immunity (Cao *et al.*, 2024). Consistent with this concept, repeated administration of the multi-target mRNA vaccine reduced bacterial burden and improved clinical outcomes in non-official agricultural field trials, supporting its therapeutic potential. However, we primarily focused on evaluating protective efficacy across multiple hosts and pathogens, and did not perform in-depth mechanistic analyses. Future studies will systematically characterize antigen-specific antibody responses, lung-resident immune cell populations, cytokine profiles, and more, with a particular emphasis on cellular immunity activated by PV in relevant animal models.

In this study, we initially developed vaccines targeting *P. multocida* using different antigen combinations and demonstrated their protective efficacy. In fact, *P. multocida* can be classified into five serotypes (A, B, D, E, and F) based on capsular polysaccharides, with serotype A exhibiting the broadest host range (Dominguez-Odio and Delgado *et al.*, 2023). Similar to our previous work on *Enterobacteriaceae*, the present study focused on cross-protection across different genera within the *Pasteurellaceae* family, rather than comparing protection across *P. multocida* serotypes. However, given that the six antigen targets included in PV are highly conserved across species within the family, their conservation within a single species is expected to be even higher. Therefore, it is reasonable to infer that PV may also provide cross-protection against multiple *P. multocida* serotypes. Definitely, this hypothesis warrants further investigation in future studies using well-defined serotype-specific challenge models.

Several limitations should be acknowledged here. The therapeutic studies in companion animals, livestock, and poultry were conducted under practical field conditions, which introduced variability in experimental design. Due to the regulatory complexity and logistical challenges associated with formal veterinary clinical trials, we adopted a customized approach based on naturally occurring infections in farm settings. As a result, limitations exist in sample size, control group design, and evaluation metrics. For example, qPCR detection of bacterial DNA does not discriminate between viable and non-viable organisms, and future studies will incorporate microbiological culture as a complementary endpoint to confirm bacteriological clearance. Additionally, possible spontaneous resolution, management factors, environmental variation, and concurrent supportive treatment, should be considered. Therefore, future studies should incorporate more standardized clinical trial designs, including appropriate randomization, blinded controls, multi-dimensional outcome assessments. Additionally, comprehensive safety assessments, including histopathological examinations of major organs, serum biochemistry panels, and local injection site tolerance assessments, should be prioritized in future studies.

Conclusions: In conclusion, we report a conserved multi-target mRNA vaccine that provides both prophylactic and therapeutic efficacy against a broad range of *Pasteurellaceae* pathogens. By leveraging conserved intracellular antigens, this strategy overcomes key limitations of traditional vaccines. Our findings highlight the feasibility of developing universal *Pasteurellaceae*

vaccines, providing a foundation for expanding host coverage, and translating the approach into potential clinical and veterinary applications.

Funding: This work was supported by the Technical Service Fund between Nanjing Chengshi (TheraRNA) Biomedical Technology Co. Ltd. and Xinyang Agriculture and Forestry University under grant number KJ(HZ)-01-2025-0123.

Data Availability: The data that support the findings of this study are available from the first author upon reasonable request.

Authors contribution: X.Y.: investigation, formal analysis, writing—original draft, funding acquisition. S.L.: data curation, writing—review and editing. Y.C.: formal analysis, writing—review and editing. J.L. and M.X.: formal analysis, data curation, methodology. Q.H., R.L., T.L., L.W., B. L. and X.L.: investigation. J.W.: writing—review and editing. S.X., T.H. and Z.C.: conceptualization, supervision, writing—review and editing, project administration. All authors interpreted the data, critically revised the manuscript for important intellectual contents and approved the final version.

Generative AI Statement: The authors declare that no generative AI or AI-assisted technologies were used in the writing or creation of this manuscript.

REFERENCES

Akcakavak G, Karatas O, Tuzcu N, *et al*., 2024. Determination of apoptosis, necroptosis and autophagy markers by real-time PCR in naturally infected Pneumonic Pasteurellosis caused by *Pasteurella multocida* and *Mannheimia haemolytica* in Cattle. Pakistan Veterinary Journal 44(2): 483-489.

Bourely C, Cazeau G, Jouy E, *et al*., 2019. Antimicrobial resistance of *Pasteurella multocida* isolated from diseased food-producing animals and pets. Veterinary Microbiology 235: 280-4.

Cao Q, Fang H, Tian H, 2024. mRNA vaccines contribute to innate and adaptive immunity to enhance immune response in vivo. Biomaterials 310: 122628.

Chen H, Ren X, Xu S, *et al*., 2022. Optimization of lipid nanoformulations for effective mrna delivery. International Journal of Nanomedicine 17: 2893-2905.

Cheng LT, Chu CY, Vu-Khac H, *et al*., 2023. Signal sequence contributes to the immunogenicity of *Pasteurella multocida* lipoprotein E. Poultry Science 102(1): 102200.

Christensen H, Bisgaard M, 2018. Classification of genera of Pasteurellaceae using conserved predicted protein sequences. International Journal of Systematic and Evolutionary Microbiology 68(8): 2692-6.

De Groot AS, Moise L, Terry F, *et al*., 2020. Better epitope discovery, precision immune engineering, and accelerated vaccine design using immunoinformatics tools. Frontiers in Immunology 11: 442.

Doan TD, Wang HY, Ke GM, *et al*., 2020. N-terminus of flagellin fused to an antigen improves vaccine efficacy against *Pasteurella multocida* infection in chickens. Vaccines (Basel) 8(2), 283.

Dominguez-Odio A, Delgado DLC, 2023. Global commercialization and research of veterinary vaccines against Pasteurella multocida: 2015-2022 technological surveillance. Veterinary World 16(5): 946-56.

Dousse F, Thomann A, Brodard I, *et al*., 2008. Routine phenotypic identification of bacterial species of the family Pasteurellaceae isolated from animals. Journal of Veterinary Diagnostic Investigation 20(6): 716-24.

Fegan JE, Waeckerlin RC, Tesfaw L, *et al*., 2024. Developing a PmSLP3-based vaccine formulation that provides robust long-lasting protection against hemorrhagic septicemia-causing serogroup B and E strains of *Pasteurella multocida* in cattle. Frontiers in Immunology 15: 1392681.

He CY, Yang JH, Ye YB, *et al*., 2022. Proteomic and antibody profiles reveal antigenic composition and signatures of bacterial ghost vaccine of *Brucella abortus* A19. Frontiers in Immunology 13: 874871.

Howlader DR, Das S, Lu T, *et al*., 2023. A protein subunit vaccine elicits a balanced immune response that protects against Pseudomonas pulmonary infection. NPJ Vaccines 8(1): 37.

Kannangara DW, Pandya D, Patel P, 2020. *Pasteurella multocida* infections with unusual modes of transmission from animals to humans: A study of 79 cases with 34 nonbite transmissions. Vector-Borne and Zoonotic Diseases 20(9): 637-51.

Kennedy SC, Johnson AJ, Bharrhan S, *et al*., 2018. Identification of Mycobacterial ribosomal proteins as targets for CD4(+) T cells that enhance protective immunity in Tuberculosis. Infection and Immunity 86(9): e00009-18

Khan M, Shi X, Wei Z, *et al*., 2024. Development of porcine reproductive and respiratory syndrome virus (PRRSV) mRNA vaccine against highly pathogenic PRRSV challenge. Pakistan Veterinary Journal 44(4): 1073-1082.

Lee J, Kang HE, Woo HJ, 2012. Protective immunity conferred by the C-terminal fragment of recombinant *Pasteurella multocida* toxin. Clinical and Vaccine Immunology 19(9): 1526-31.

Liu R, Xu S, Liu S, *et al*., 2025. Next-generation mRNA vaccines eliciting robust protection against multidrug-resistant Enterobacteriaceae. NPJ Vaccines 11(1): 24.

Massacci FR, Magistrali CF, Cucco L, *et al*., 2018. Characterization of *Pasteurella multocida* involved in rabbit infections. Veterinary Microbiology 213: 66-72.

Michael GB, Bosse JT, Schwarz S, 2018. Antimicrobial resistance in Pasteurellaceae of veterinary origin. Microbiology Spectrum 6:10.1128.

Mostaan S, Ghasemzadeh A, Sardari S, *et al*., 2020. *Pasteurella multocida* vaccine candidates: A systematic review. Avicenna Journal of Medical Biotechnology 12(3): 140-7.

Moustafa DA, Lou E, Schafer-Kestenman ME, *et al*., 2024. *Pseudomonas aeruginosa* elongation factor-Tu (EF-Tu) is an immunogenic protective protein antigen. Vaccine 42(26): 126476.

Munir A, Li C, Kolenda R, *et al*., 2025. Exploring the diversity and dissemination dynamics of antimicrobial resistance genes in Enterobacteriaceae plasmids across varied ecological niches. Pakistan Veterinary Journal 45(2): 662-672.

Pardi N, Krammer F, 2024. mRNA vaccines for infectious diseases advances, challenges and opportunities. Nature Reviews Drug Discovery 23(11): 838-61.

Park PG, Fatima M, An T, *et al*., 2024. Current development of therapeutic vaccines for the treatment of chronic infectious diseases. Clinical and Experimental Vaccine Research 13(1): 21-7.

Peng Z, Liang W, Wang F, *et al*., 2018. Genetic and phylogenetic characteristics of Pasteurella multocida isolates from different host species. Frontiers in microbiology 9: 1408.

Peng Z, Wang X, Zhou R, *et al*., 2019. *Pasteurella multocida*: genotypes and genomics. Microbiology and Molecular Biology Reviews 83:10.1128.

Piorunek M, Brajer-Luftmann B, Walkowiak J, 2023 *Pasteurella multocida* infection in humans. Pathogens 12(10): 121.

Rijkers GT, Weterings N, Obregon-Henao A, *et al*., 2021. Antigen presentation of mRNA-Based and virus-vectored SARS-CoV-2 vaccines. Vaccines (Basel) 9(8): 848.

Seo J, Pyo H, Lee S, *et al*., 2009. Expression of 4 truncated fragments of *Pasteurella multocida* toxin and their immunogenicity. Canadian Journal of Veterinary Research 73(3): 184-9.

Tesfaye AB, Werid GM, Tao Z, *et al*., 2025. Advances in *Pasteurella multocida* vaccine development: from conventional to next-generation strategies. Vaccines (Basel) 13(10): 1034.

Tian Y, Hu D, Li Y, *et al*., 2022. Development of therapeutic vaccines for the treatment of diseases. Molecular Biomedicine 3(1): 40.

Walker RI, 2025. Conserved antigens for enteric vaccines. Vaccine 50: 126828.

Weerarathna IN, Doelakeh ES, Kiwanuka L, *et al*., 2024. Prophylactic and therapeutic vaccine development: advancements and challenges. Molecular Biomedicine 5(1): 57.

Whitley J, Zwolinski C, Denis C, *et al*., 2022. Development of mRNA manufacturing for vaccines and therapeutics: mRNA platform requirements and development of a scalable production process to support early phase clinical trials. Translational Research 242: 38-55.

Wu MC, Lo YT, Wu HC, *et al*., 2021. Cross-protection of recombinant Pasteurella multocida toxin proteins against atrophic rhinitis in mice. Research in Veterinary Science 137: 138-43.

Xu S, Li J, Xu M, *et al*., 2025. A novel trivalent BVDV mRNA vaccine displayed by virus-like particles eliciting potent and broad-spectrum antibody responses. Vaccines 3(7): 691.

Xu S, Qi G, Liu R, *et al*., 2025. Development of a novel-ionizable-lipid-based mRNA vaccine for broad protection against *Streptococcus pneumoniae*. Molecular Therapy - Nucleic Acids 36(4): 102699.

Yang W, Li M, Zhang C, *et al*., 2022. Pathogenicity, colonization, and innate immune response to *Pasteurella multocida* in rabbits. BMC Veterinary Research 18(1): 416.